Microchemical Journal 154 (2020) 104654

Contents lists available at ScienceDirect

Microchemical Journal

journal homepage: www.elsevier.com/locate/microc

A modified sensitive carbon paste electrode for 5-fluorouracil based using a composite of praseodymium erbium tungstate

Mehdi Rahimi-Nasrabadi[a,b,*], Farhad Ahmadi[c,d,*], Hana Beigizadeh[e], Meisam Sadeghpour Karimi[e], Ali Sobhani-Nasab[f,g], Yvonne Joseph[h], Hermann Ehrlich[h], Mohammad Reza Ganjali[e,i]

[a] Chemical Injuries Research Center, Systems Biology and Poisonings Institute, Baqiyatallah University of Medical Sciences, Tehran, Iran
[b] Faculty of Pharmacy, Baqiyatallah University of Medical Sciences, Tehran, Iran
[c] Razi Drug Research Center, Iran University of Medical Sciences, Tehran, Iran
[d] Department of Medicinal Chemistry, School of Pharmacy-International Campus, Iran University of Medical Sciences, Tehran, Iran
[e] Center of Excellence in Electrochemistry, University of Tehran, Tehran, Iran
[f] Social Determinants of Health (SDH) Research Center, Kashan University of Medical Sciences, Kashan, Iran
[g] Core Research Lab, Kashan University of Medical Sciences, Kashan, Iran
[h] IESEM, TU Bergakademie, Germany
[i] Biosensor Research Centre, Endocrinology & Metabolism Molecular and Cellular Research Institute, Tehran University of Medical Sciences, Tehran, Iran

ARTICLE INFO

Keywords:
Praseodymium erbium tungstate
Modified carbon paste electrode
Anticancer drug
5-fluorouracil
Square wave voltammetry (SWV)

ABSTRACT

This paper describes the modification of a modified carbon paste electrode (CPE) using nanoparticles of praseodymium erbium tungstate (Pr:Er). The modified electrode was used for the sensitive voltammetric detection of an anticancer drug (5-fluorouracil (5-FU)) using. The modified-CPE was evaluated using cyclic voltammetry (CV), square wave voltammetry (SWV) and electrochemical impedance spectroscopy (EIS) and the resulting data showed the irreversible 5-fluorouracil oxidation peak around 1.0 V vs. Ag/AgCl. Some key parameters such as pH, the amount of the modifier, potential amplitude, step potential and frequency were studied and optimized. The square wave voltammetry (SWV) analytical calibration curve was linear in the range of 0.01–50 μM, with a detection limit of 0.98 nM analyses. The electron transfer coefficient (α) was also determined to be 0.76. The analyte concentration was also determined in pharmaceutical formulations and recovery percentages were found to be in the range of 96–102%. The sensor had good reproducibility and repeatability with acceptable RSD values of 3.6%, and 1.02% and a rather long-term stability of around one month. The as-synthesized nanoparticles were also characterized using FESEM, TEM, FTIR and XRD techniques.

1. Introduction

Treating cancer is a prevailing issue and many studies have been performed in the area of treating or preventing cancer and oxidative stress. Also treating wounds to prevent the effects of chronic pre-cancerous effect of inflammation have been subjects of different research projects [1–3]. In effect, the determination of the concentration of anticancer agents in body fluids of patients has become very important.

5-fluorouracil is anti-metabolite that inhibits the essential biosynthetic processes and also interacts with DNA and RNA, inhibiting usual activity. Therefore, it widely used in treating various kinds of cancers including aerodigestive tract, colorectal, and breast cancers. The response rates and survival 5-FU in neck, breast and head cancers of improved when it was used with other chemotherapeutic drugs [4]. The greatest efficiency of the drug was observed in the case of colorectal cancer [5, 6].

As 5-FU has several sever side-effects apart from its expected properties, its determination in pharmaceuticals and biological fluids is of interst specially in the area of oncology [7]. Various analytical methods such as liquid chromatography [8, 9], GC-MS [10] and capillary electrophoresis [11] have been used for determining 5-FU in various samples. Although these methods have great performance, they have several disadvantages including high time and cost requiredments, complex sample-preparation procedures, and the need for highy skilled operators [12], and hence the development of simpler, faster and more economic analytical techniques for 5-FU is always a need.

Due to the high selectivity, sensitivity, short time response and econemic advantes of electrochemical techniques, they are considered

* Corresponding authors.
E-mail addresses: rahimi@bmsu.ac.ir (M. Rahimi-Nasrabadi), fahmadi@kums.ac.ir (F. Ahmadi).

https://doi.org/10.1016/j.microc.2020.104654
Received 8 April 2019; Received in revised form 24 December 2019; Accepted 16 January 2020
Available online 16 January 2020

as alternative methods for the aforementioned analyses [13–15]. Specifically, chemically-modified electrodes (CMEs) constitute very attractive optionswith high sensitivity, selectivity and the analytical performance [6]. From the various working electrodes that can be modified, carbon paste electrodes (CPEs) have received extensive attention, because of advantages like ease of preparation, biocompatibility, high stability, low cost, surface renewability, and wide working potential windows. In addition, the easy incorporation of modifiers in the formulation of carbon pastes adds to their appeal [16–18]. The selectivity and performance of modified carbon paste electrodes (mCPEs) to analytes is highly dependent on the properties of the modifier.

Nanostructure modified sensors have been developed extensively as a promising approach to facilitate the electron transfer rate between electrode and biomolecules [19,20]. Lanthanides or f-block metallic elements, as an instance of such modifiers are known to have specific physical, nuclear, photogenic, and magnetic properties and are widely used in metallurgy, agricultural and ceramic industry. Like many different nanomaterials, nanostructures of lanthanide compounds have interesting electro-catalytic properties and can be used as modifier in sensors [21–30].

In the light of the aforementioned, the present work was focused on developing a novel voltammetric sensor for 5-FU using a Pr:Er-modified mCPE. The electrode was used in the determination of 5-FU in pharmaceutical formulations through SWV experiments in optimal pH, modifier composition, and SWV parameters. Moreover, the method based on the developed mCPE, and its reproducibility and stability, were studied and validated

2. Materials and techniques

2.1. Chemicals

Doublly-distilled water (DDW) and analytical grade reagents were used throughout the experiments. High quality paraffin oil, the graphite powder, $K_4[Fe(CN)_6].3H_2O$, $K_3[Fe(CN)_6]$, praseodymium nitrate hexahydrate, erbium nitrate hexahydrate, sodium tungstate dihydrate, and other analytical grade chemicals were obtained from Merck Co. Standard stock 1.0 mM 5-FU solutions were freshly prepared using a 0.1 M phosphate buffer solutions (PBS), prepared using suitable quantities of standard solutions of NaH_2PO_4 and Na_2HPO_4, and adjusting the pH using NaOH solutions.

2.2. Apparatus

Electrochemical tests were performed under ambient conditions, using a conventional three-electrode setup. The reference electrode used was a saturated Ag/AgCl electrode, and a graphite electrode was used as the auxiliary electrode. Modified and unmodified CPEs were used as the working electrode. To study the qualities of the modified electrodes cyclic voltametry (CV) and electrochemical impedance spectroscopy (EIS) analyses were performed. Further the 5-FU was analyzed in various samples through square wave voltammetry (SWV) experiments on a PalmSens instrument. The properties of the inorganic additive were evaluated by field emission scanning electron microscopy (FESEM) studies on a Hitachi S-4160 instrument. A Zeiss EM900 transmission electron microscope was used for obtaining the TEM images. For the purpose of the analyses, the sample was deposited on a carbon-coated Cu grid. X-ray powder diffraction (XRD) analyses were conducted on a Rigaku D/Max 2500 V instrument with a graphite monochromator and a Cu target. The Fourier transform infrared (FT-IR) spectroscopy experiments in the wavenumber range of 4000–500 cm^{-1} were performed using a Perkin-Elmer spectroscope and the KBr pellet technique.

2.3. Synthesis of the Pr:Er nanoparticles

Praseodymium erbium tungstate nanoparticles (Pr:Er NPs) were synthesized through a hydrothermal reaction between a the corresponding solutions of the cations and anion as reported before [31]. To this end, a mixture of praseodymium (Pr) and erbium (Er) nitrate solutions (0.01 M of each cation) at a 1:1 molar ratio were mixed with an appropriate amount of a 0.01 M solution of sodium tungstate. The solution of the cations was added to that of the anion under stirring and the resulting suspension was transferred into a Teflon-lined stainless style autoclave and heated at 170 °C for 24 h using an electric oven. Then, the resulting precipitate was centrifuged, separated and repeatedly washed using DDW and then ethanol several times and eventually dried at 80 °C for 120 min. Next the product was calcined in an electrical furnace at 600 °C for another 120 min.

2.4. Modified and unmodified CPEs

To prepare the CPEs, 0.1 g of the paste was prepared using a 70/30 (w/w) mixture of paraffin oil (binder) and graphite powder. Next, a quantity of the paste was tightly pressed into a 3-mm (I.D) glass tube and a copper wire was inserted into it from the opposite end of the tube to act as a solid contact. The surface of each CPE was smoothed through rubbing their outer surface on a piece of paper before use.

The modified CPEs were prepared in the same fashion, except for the fact that 3 to 10% wt. of the Pr:Er nanoparticles were added to the graphite powder in the initial step.

2.5. Preparation of the real samples

5-FU 50.0 mg mL^{-1} injections were purchased from a local drugstore, and based on the labeled content, a known volume of the liquid was accurately pipetted, diluted using 0.01 M PBS pH = 7.0 to obtain a 1.0×10^{-2} M solution. This sample was next analyzed through standard addition voltammetric analyses.

In the case of the urine samples, 1 mL of the specimens was diluted using PBS (pH = 7) in a 100 ml volumetric flask and analyzed after adding known amounts of a 5FU solution, before SWV analyses under optimal conditions.

Human blood was obtained from a healthy volunteer, allowed to clot at ambient conditions, and then centrifuged at 1500 rpm for 10 min. Then 2.5 ml of the supernatant (serum) was diluted using 0.1 M PBS (pH = 7) in a 25 mL flask and then analyzed.

3. Results

3.1. Characterization of the Pr:Er nanoparticles

As-synthesized Pr:Er nanoparticles were characterized by different techniques. The morphology and dimensions of the Pr:Er nanoparticles were evaluated by field emission scanning electron microscopy (FESEM) and transmission electron microscopy (TEM). Fig. 1A illustrates the FESEM image obtained for the nanoparticles and the TEM image can be seen in Fig. 1B. The latter demonstrates that the nanoparticles are homogeneous spheres. The particle size distribution of the nanoparticles (Fig. 1C) indicates an average particle diameter of 35 ± 10 nm. To evaluate the composition of the product its EDX pattern was acquired. Fig. 1d shows the typical EDX pattern of synthesized nanoparticles. The EDX pattern showed that the product is highly pure, and the average atomic percentage ratio of Pr, Er, W and O is about 10.3:12.2:50.8:26.7, respectively.

The FT-IR spectra of the Pr:Er nanoparticles are presented in Fig. 2. The stretching vibrations of O—H groups of the interlayer and surface water molecules are reflected by two peaks at 3416 and 1628 cm^{-1} [32–35]. The absorption peaks around 919, 824 and 629 cm^{-1} were attributed to the stretching and bending of W—O—W and O—W—O

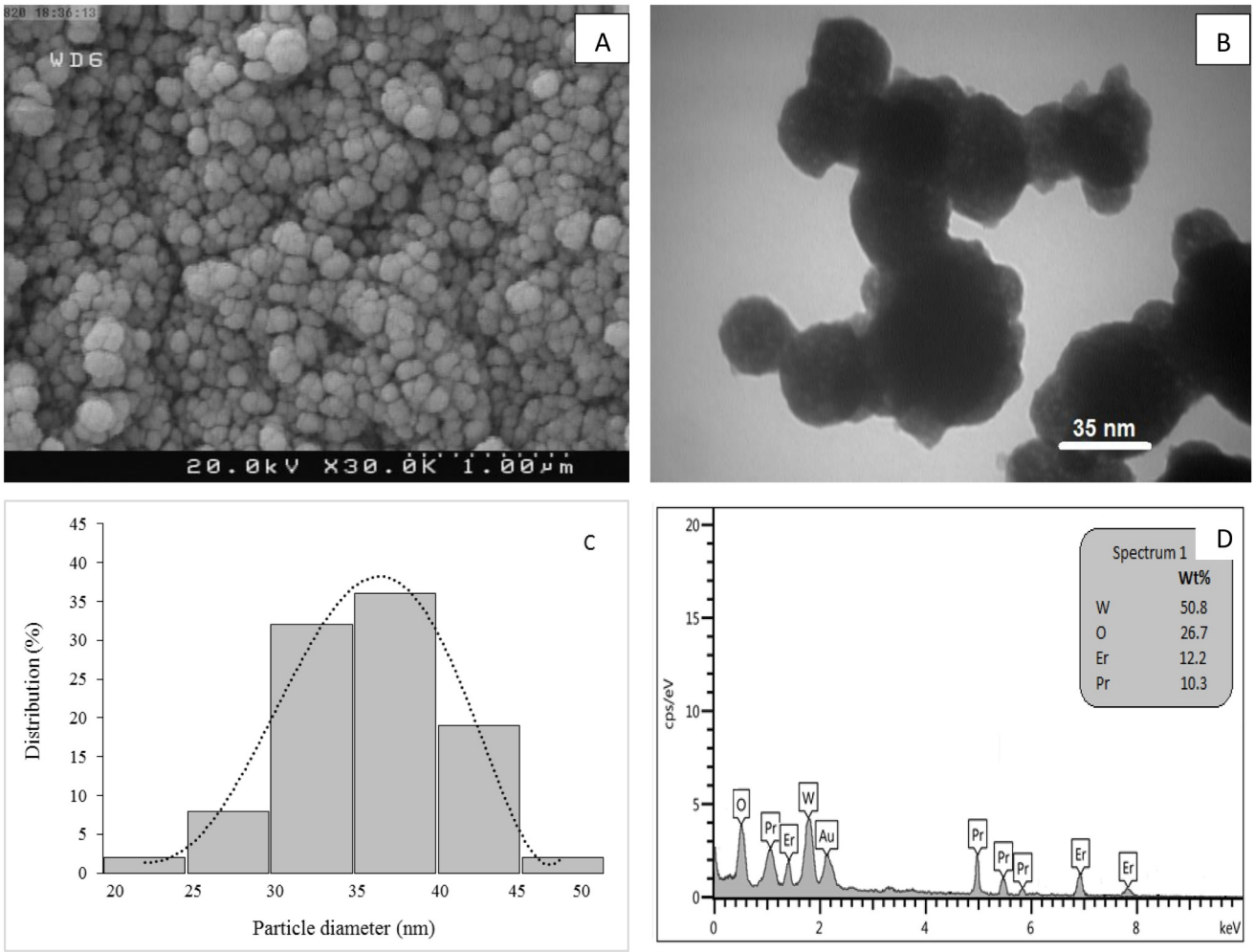

Fig. 1. (A) FESEM image of Pr:Er nanoparticles, (B) TEM image of Pr:Er nanoparticles, (C) Particle size distribution (200 particles), (D) EDS pattern of Pr:Er nanoparticles.

bonds [31].

The composition of the Pr:Er nanoparticles was evaluated through XRD analyses (Fig. 3) and the indexed diffraction peaks in the results were found to comply with the reference XRD patterns of monoclinic praseodymium tungstate oxide (JCPDS Card No. 021-0739), and orthorhombic structure of erbium tungstate oxide (JCPDS Card No. 038-0102). The average crystalline size of the nanoparticles was calculated by the Debye-Scherrer equation [36–39]:

$$D = \frac{0.9\lambda}{\beta\ \mathrm{Cos}\theta}$$

where λ (X-ray radiation wavelength) is 0.154059 nm, β represents the modified band broadening, and θ shows the so-called Bragg's angle [32, 40].

Based on the results the average crystal size of Pr:Er particles was determined to be around 36 nm.

3.2. Electrochemical characterization experiments

The electron transfer properties of Pr: Er/CPE, and bare CPE were evaluated through CV and EIS experiments using a 5.0 mM $[Fe(CN)_6]^{3-}/[Fe(CN)_6]^{4-}$ solution as a redox probe and the results are presented in Fig. 4. The CVs in Fig. 4A, illustrate a quasi-reversible behavior on the part of both electrodes. Clearly, in the case of the mCPE, the peak currents were stronger while the peak-to-peak potential separation (ΔEp) was lower. This enhanced behavior was attributed to the presence of the Pr:Er modifier in the CPE composition, which enhances the electron transfer kinetics and reversibility of the modified electrode due to the enhanced surface area.

The Nyquist plots (EIS) of the modified and untreated CPEs as illustraated in Fig. 4B, comply with the voltammetric results. Given that the continuous reductions of the electron transfer resistance (Rct) values, obtained using a proper equivalent circuit, were 3907.05 Ω for the untreated CPE, and 58.8955 Ω for the Pr:Er/CPE, it can be said that the electron transfer between the $[Fe(CN)_6]^{3-}/[Fe(CN)_6]^{4-}$ redox probe and the electrode surface is faster in the case of the modified electrode. This indicates that the incorporation of Pr:Er into the CPE comosition effectively enhanced the conductivity of the electrode, facilitating electron transfer phenomena.

Using the Randles-Sevcik's equation, the electroactive surface areas of the modified and unmodified CPEs were determined:

$$I_p = (2.69 \times 10^{-5})\ n^{3/2} A\ D^{1/2} C\ \nu^{1/2}$$

In this equation I_p and n are the peak current and sum of electrons transferred; A represents the electroactive surface area (cm^2); D and C are the diffusion coefficient (7.6×10^{-6} cm^2 s^{-1} for 5 mM $[Fe(CN)_6]^{3-}$ ion in KCl 0.1 M), and concentrations of the electroactive species (mol cm^{-3}), and ν represents the potential scan rate (Vs^{-1}) [41, 42].

For $n = 3$, the respective values of the average active surface areas of CPE and Pr:Er/CPE were determined to be 0.045 and 0.093 cm^2, respectively, indicating that the Pr:Er nanocomposite could enhance the

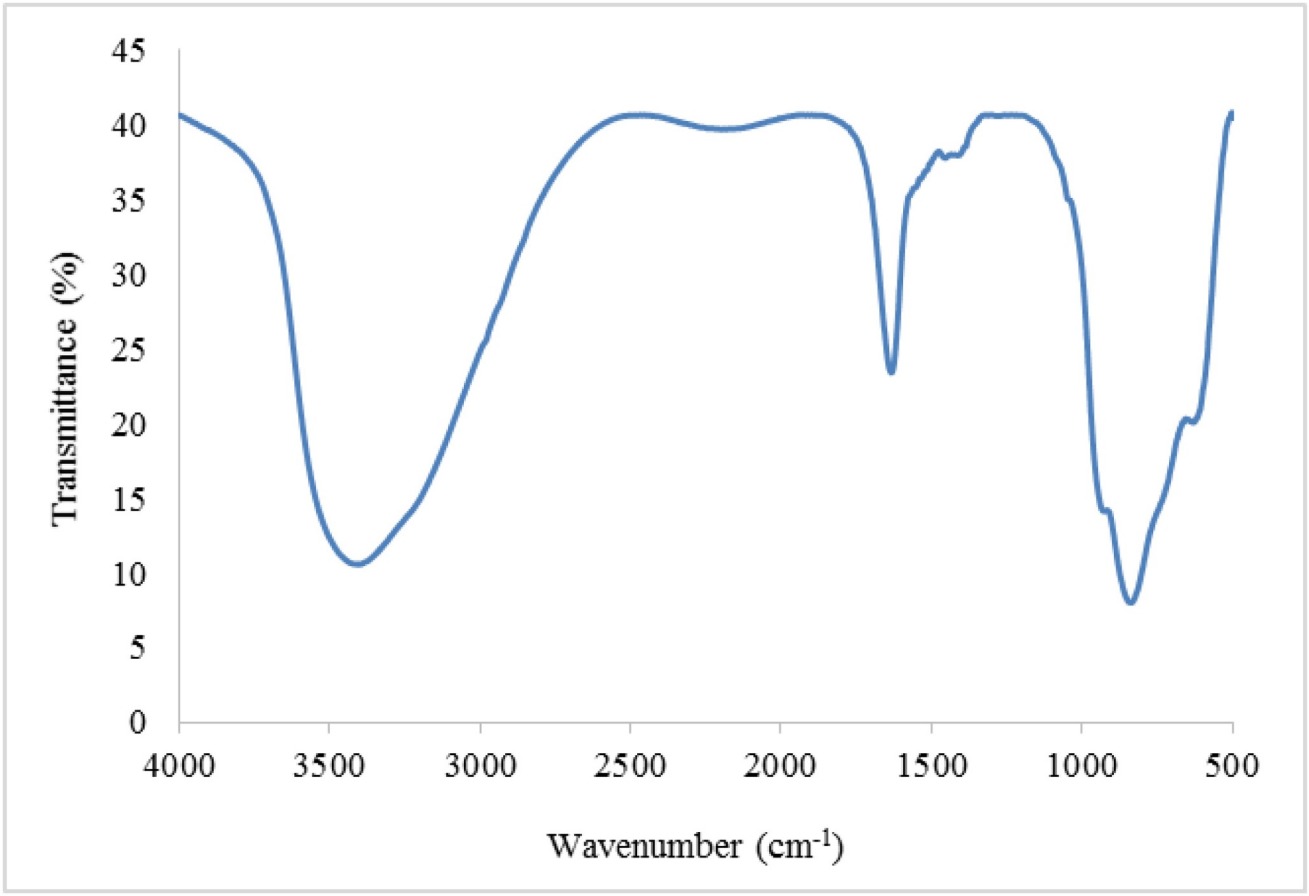

Fig. 2. FTIR spectrum of Pr:Er nanoparticles.

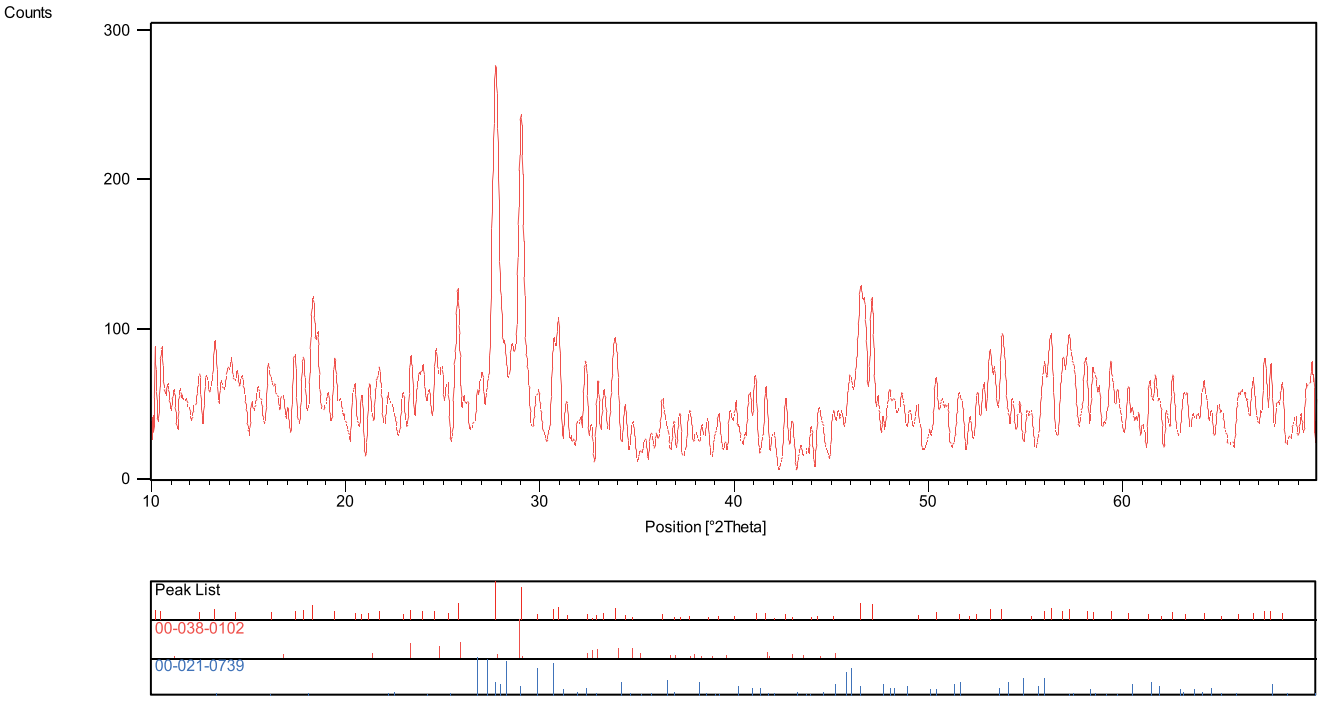

Fig. 3. XRD pattern of synthesized Pr:Er nanoparticles.

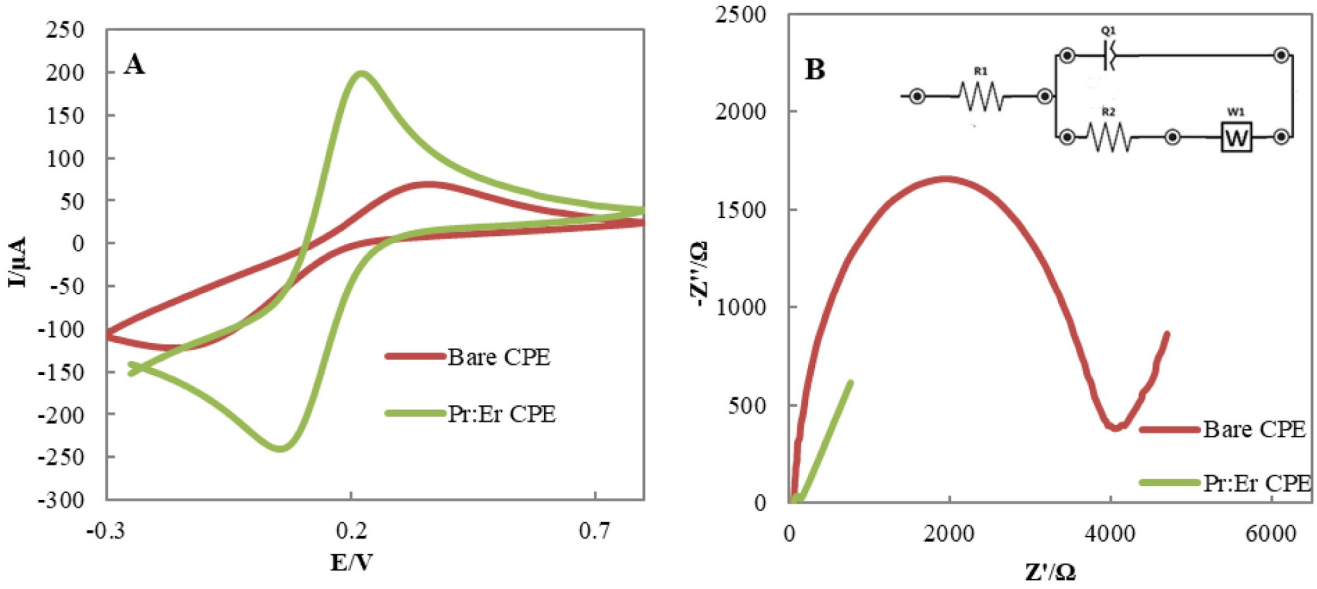

Fig. 4. (A) Cyclic voltammogram, (B) Nyquist plots of bare and Pr:Er/CPE in 5.0 mM $K_4Fe(CN)_6/K_3Fe(CN)_6$ and 0.1 M KCl at 100 mVs^{-1}.

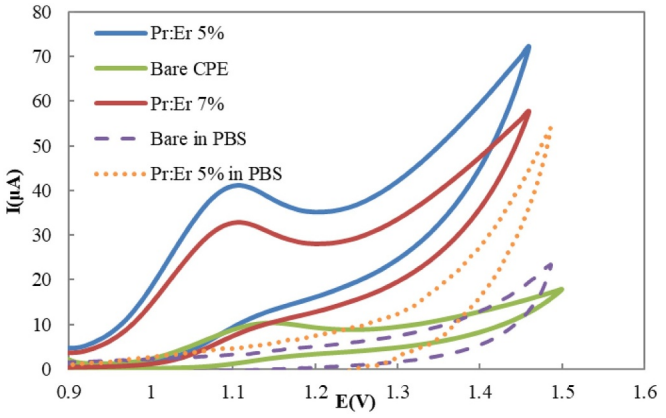

Fig. 5. CVs obtained in absence of 5-FU, bare (dash line) and modified (dotted line), bare CPE (green line), 5% Pr:Er/CPE (blue line) and 7% Pr:Er/CPE (red line) working electrodes in a 1.0 mM solution of 5-FU in 0.01 M PBS solutions (pH = 7.0), at 100 mVs^{-1}. (For interpretation of the references to color in this figure legend, the reader is referred to the web version of this article.)

availability of effective area of the electrode surface.

3.3. Voltammetric analyses

The performance of the Pr:Er/CPE was evaluated by CV experiments using bare and mCPEs containing 5% of Pr:Er (5% Pr:Er/CPEs) in a 1.0 mM solution of 5-FU in 0.01 M PBS (pH = 7.0). The experiments were performed at 100 mV/s (Fig. 5). Both bare and modified CPEs showed an oxidation peak at around 1.15 and 1.10 V respectively, with no cathodic peaks during the reverse scan. Yet, the modified electrodes showed higher sensitivity and stability, as well as higher peak currents, supporting the higher electrocatalytic activity of the modified electrode towards 5-FU. However, by further increasing the amount of the modifier to 7% in the CPE composition, the signal decreased in comparison to that 5% Pr:Er/CPE.

No characteristic peaks were observed in blank PBS, using the modified electrode (Fig. 5), indicating that PBS is inert.

3.4. Effect of the potential scan rate

The effect of scan rate on the results was studied through recording CVs in a 1.0 mM of 5-FU solution using Pr:Er/CPE while changing the scan rate within the range of 10–900 mVs^{-1} (Fig. 6A). It can be seen that the oxidation currents increased and the peak potential moved to more positive values as the scan rate increased. Figure (6B) illustrates that the anodic peak currents (I_p) change linearly with the square root of scan rate ($\nu^{1/2}$) in this window, which indicates that the electrochemical process is diffusion-controlled.

According to the Laviron's equation [43], and using the changes in the anodic peak potentials versus the logarithm of scan rate, one can determine the charge transfer coefficient (α) and the heterogeneous rate constant (k) of a reaction. The Laviron's equation is as follows:

$$Ep = E^0 + (RT/\alpha nF)\,[\ln(RTk_s/\alpha nF) - -\ln\upsilon]$$

Where E^0 is the formal potential, α is the electron transfer coefficient, υ is the scan rate, k_s is the heterogeneous rate constant of the surface reaction and n is the electron transfer numbers. The E^0 value can be obtained from the intercept of *E*p vs. υ plot on the ordinate by extrapolating the line to (υ = 0). The slope obtained from Figure (6C) (i.e. changes in the E_p with the logarithm of the scan rate) gives α_a, knowing that the slope of the rectilinear part of the plot is 2.303RT/ (1 – α)nF for anodic peaks. Given that the oxidation of 5-FU has been reported to be a two-electron process before [44], the anodic transfer coefficient (α_a) was calculated to be 0.76. The value of the heterogeneous rate constant (k_s) was determined to be 1.35 s^{-1}.

3.5. Effect of pH

pH of the analysis media is an important factor in determining the electrochemical behavior of the analyte and the sensor since it affects the mechanism of the electrochemical reaction of the analyte. In this study, the effect of pH was assessed using PBSs with various pH values ranging from 3.0 to 9.0 in the voltammetric studies (Fig. 7). The results showed that increasing the pH shifted the peak potential in the negative direction. This reflects the involvement of H^+ in the electrochemical reaction. Further increasing the pH from 3.0 to 7.0 increased the peak current, while the currents decreased beyond this range.

In this light a pH of 7.0, which is a biological pH, was found to be the optimal value. All other experiments were performed at this pH. The anodic peak potentials changed linearly with pH according to the below linear regression equation:

$$Epa\ (V) = 1.5464 - 0.0596\ pH\ (R^2 = 0.995)$$

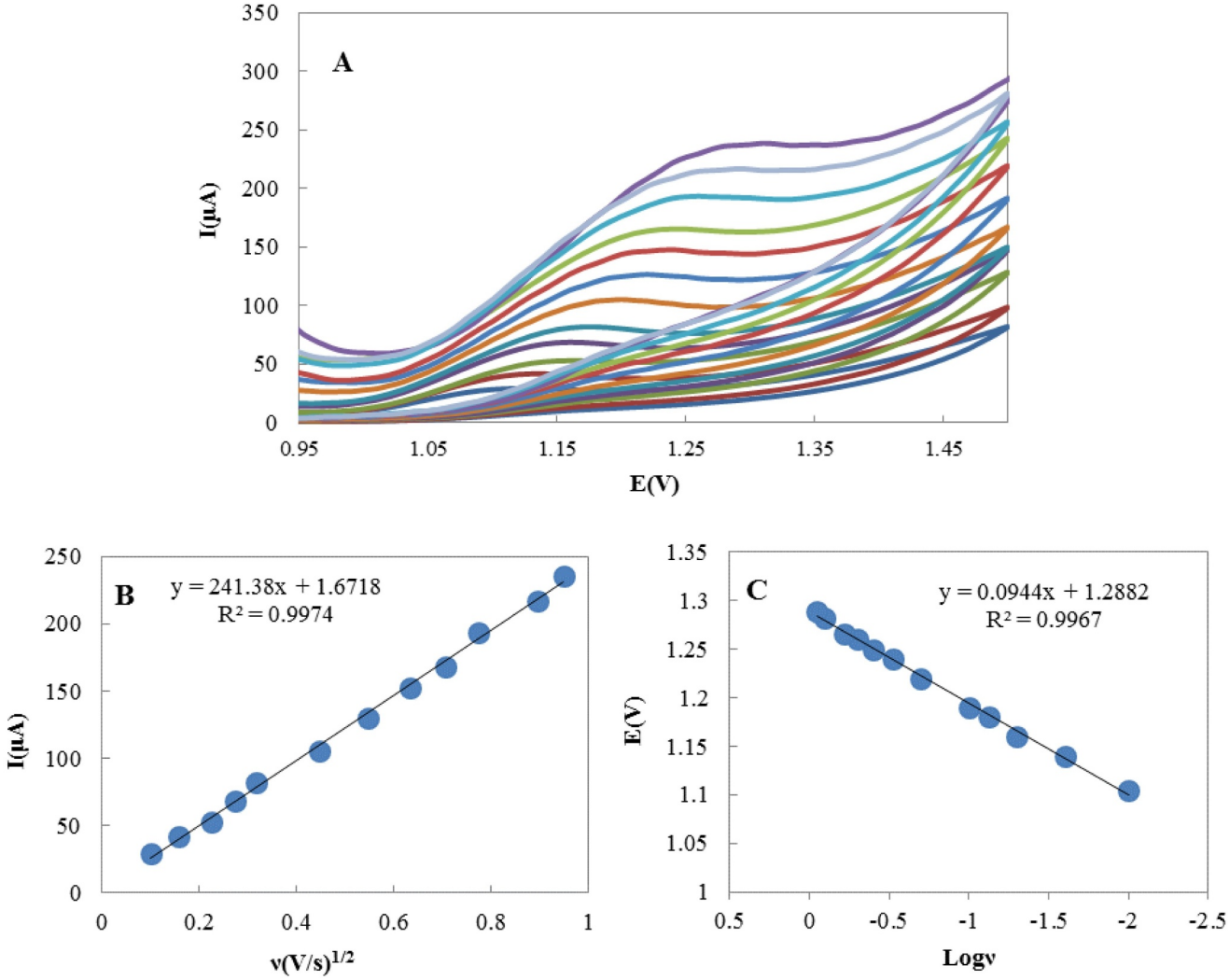

Fig. 6. (A) CVs obtained using Pr:Er/CPE in a 0.1 mM of 5-FU in 0.01 M PBS (pH = 7.0), at 0.01 to 0.9 Vs^{-1}, from inside to outside the plots, (B) Variations of the peak current versus square root of scan rates, (C) Variation of E_p versus the logarithm of the scan rate.

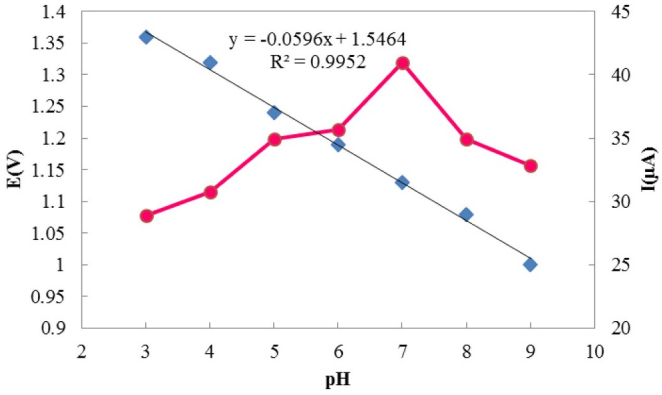

Fig. 7. The plot of pH vs. peak current and peak potentials for Pr:Er/CPE at different pH values, scan rate 100 mVs^{-1}.

The slope of this line (0.0596 VThis reflects the involvement of pH^{-1}) indicates that the number of electrons and H^+ ions involved in the reaction are equal.

3.6. Optimizing the SWV experiments

Square wave voltammetry, as a sensitive direct technique for trace analyses of various compounds, is a conventional tool in the analysis of pharmaceuticals. The SWV peak current is influenced by different interrelated instrumental factors like SW frequency (f_{sw}), step potential (Δs) and SW amplitude (E_{sw}). To determine the optimal values of these parameters, changes in the peak current for a 1.0 mM 5-FU in PBS (0.01 M, pH = 7.0), upon changing each factor were recorded and the findings are presented in Fig. 8. Based on these observations, an amplitude of 70.0 mV (Fig. 8A), an f_{sw} of 40.0 Hz (Fig. 8B), and a ΔS of 8.0 mV (Fig. 8C) were found to be the optimal values.

3.7. Reproducibility, repeatability, and stability

The reproducibility of the analytical responses obtained with the developed modified CPE was evaluated using 5 electrodes to analyze a 1.0 mM 5-FU solution on 5 different days. The relative standard deviation (RSD) calculated for the result of these experiments was 3.6%, which reflects the reproducibility of the electrodes. Under the same conditions, the repeatability of the results was tested 5 times in one single day, and the calculated RSD was 1.02%. All measurements were performed after renewing the electrode surfaces by abrasion and under ambient conditions, the electrodes showed long-term stability (almost one month).

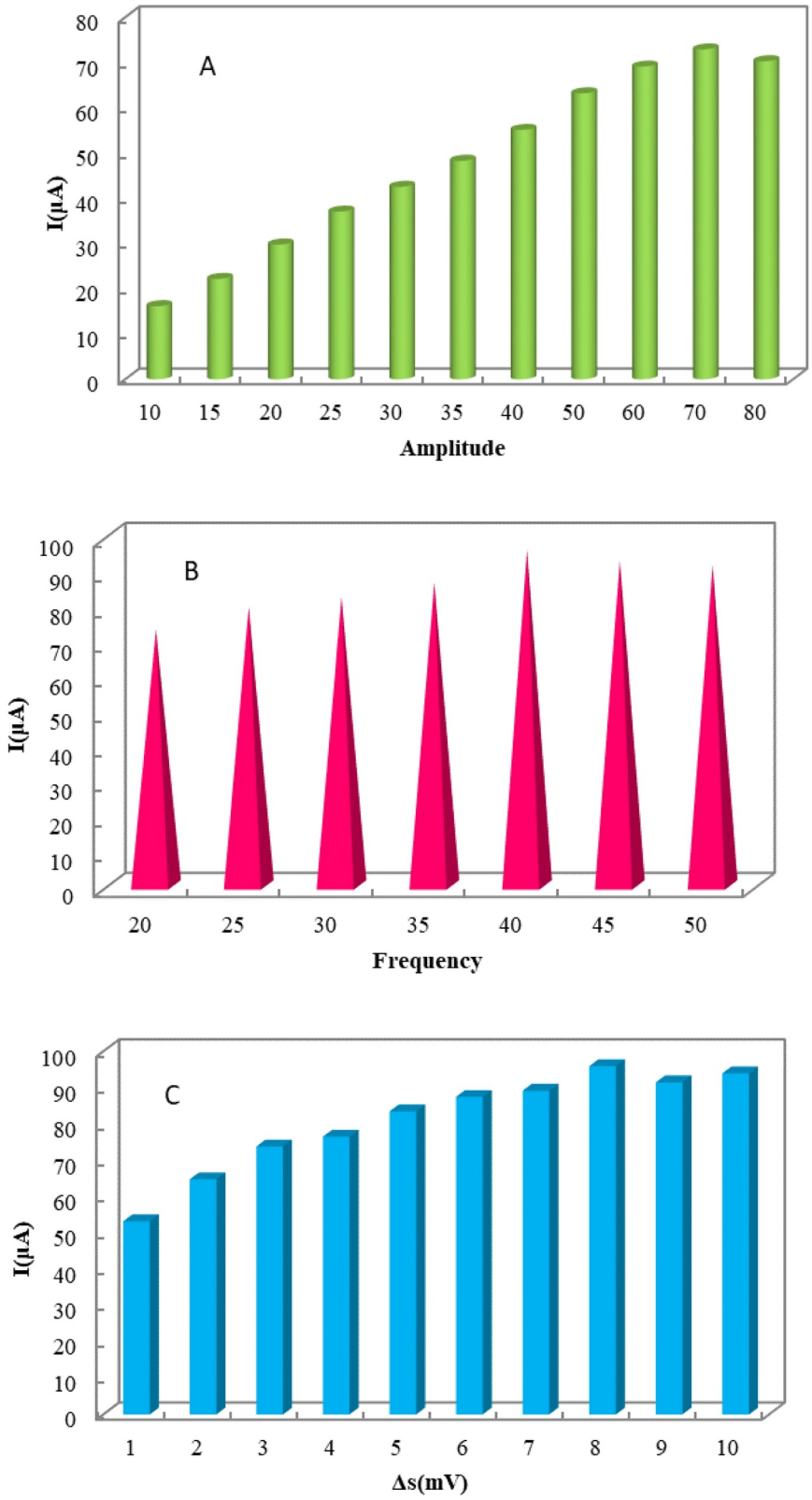

Fig. 8. The optimization of amplitude (A), frequency (B) and the step potential, (C) for 1.0 mM 5-FU in PBS, pH 7.0, at Pr:Er/CPE.

3.8. Calibration curve

SWV analyses were performed under the optimal conditions. According to Fig. 9A the peak currents increased with increasing the 5-FU concentration in the range of 0.01 to 50 μM (Fig. 9B). The detection limits of the method at 3SD/b (SD: standard deviation (SD) for an intercept and b - the slope of the linear regression equation). The calculated LOD was 0.98 nM 5-FU, which is much less than the results reported in previous works (Table 1).

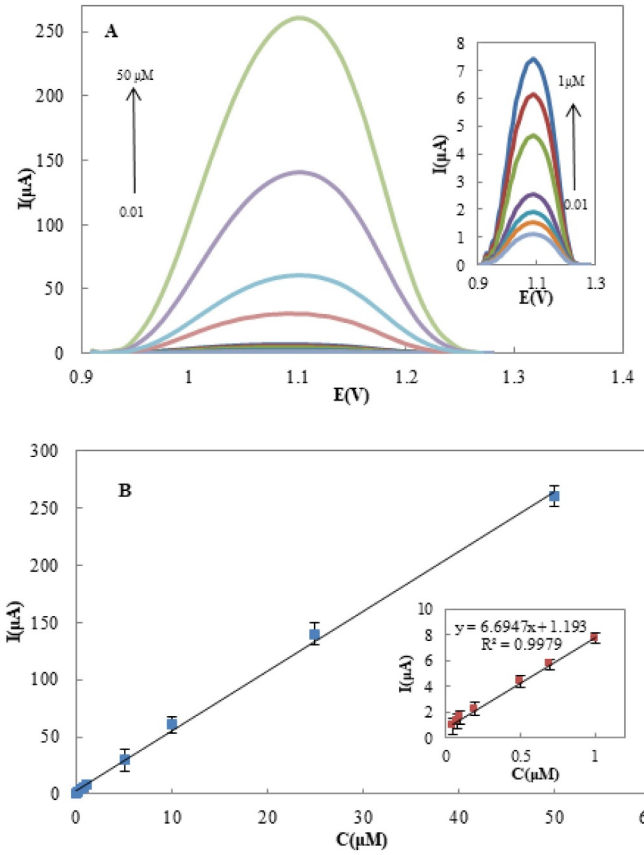

Fig. 9. (A) Square wave voltammograms and (B) Calibration curve observed for 0.01–50.0 μM 5-FU (from inside to outside) in 0.01 M phosphate buffer (pH 7.0) at Pr:Er/CPE.

Table 1
Comparison of the efficiency of previous work in the electrochemical determination of 5-FU.

Electrode	Method	LOD (nM)	Ref
BTB/MWNT/GCE	CV	270	[45]
CETAB/GCE	DPV	20.0	[46]
Au Nps/SPE	SWV	76.9	[47]
$ZnFe_2O_4$/IL/ CPE	SWV	70.0	[48]
Au Nps-PFR/CPE	DPV	66.0	[6]
MTB/CPE	DPV	2.04	[44]
Pr:Er/CPE	SWV	0.98	This work

Table 2
Influence of potential excipients on the voltammetric response of 1.0 μM 5-FU.

Excipients	Concentration (mM)	Signal change (%)
D-Glucose	0.1	2.83
Citric acid	0.1	−1.38
Gum acacia	0.1	3.52
Dextrose	0.1	2.03
Lactose	0.1	3.58
Sucrose	0.1	1.74
Starch	0.1	1.07
Uric acid	0.1	−2.15
Dopamine	0.1	1.47
Xanthine	0.1	−0.35

3.9. Effect of interfering species

The effects of some common pharmaceutical species on the response of the developed electrode were studied, considering that relative errors

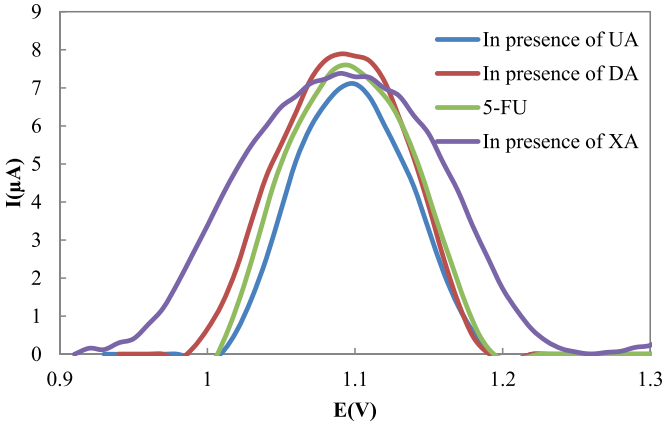

Fig. 10. Square wave voltammograms of 1.0 μM 5-FU in presence of 0.1 mM dopamine (DA), uric acid (UA) and xanthine (XA) in 0.01 M phosphate buffer (pH 7.0) at Pr:Er/CPE.

of less than 5% in the peak current as being negligible. The test solutions were a 1.0 μM 5-FU solution spiked with different amounts of the tested interfering species under the similar conditions. Based on the results, 100 folds of dopamine (DA), uric acid (UA) and xanthine (XA), citric acid, dextrose, D-glucose, gum acacia, lactose, starch, and sucrose did not cause considerable interferences in the results of 5-FU (Table 2), indicating that the procedures can be confidently used for the analysis in the presence of rather high amounts of these commonly occurring species. Fig. 10 shows the interference study of dopamine (DA), uric acid (UA) and xanthine (XA) on 5-FU determination.

3.10. SWV analysis of 5-FU in pharmaceutical formulations

Using samples of commercial 5-FU injections, as described above SWV analyses were performed based on standard addition and each experiment was repeated 5 times. The recorded recovery values are presented in Table 3. These values were in the range of 96.4 to 102.4%, indicating that the sample matrix did not significantly influence the response. The data further complied with the content of the samples based on the labeled amounts. These results clearly indicate that the devloped electrode is an efficient tool for the analysis of 5-FU in pharmaceutical amples.

3.11. Analysis of 5-FU in urine and human serum

The urine and plasma samples were prepared as desribed earlier and were then spiked with known quantitites of 5-FUand the analyses were pefroemd using calibration graphs. The results (Table 4) reflected high recovery (97.0 to 100.8%) and low RSD values (0.8–1.2%), indicating the accuracy and precision of the analyses. Some of the samples were analyzed by a reference HPLC technique [49] for validity evaluationsand the results showed good accuracyand percision.

Table 3
Results for the analysis of 5-FU in injection with the Pr:Er/CPE by SWV.

Labeled (mg mL^{-1})	50
Determined (mg mL^{-1})[a]	49.4
RSD (%)	0.89
Added (μg mL^{-1})	11.6
Found (μg mL^{-1})[a]	11.2
Recovery (%)	98.6
RSD (%)	0.63

Table 4
Results for the analysis of 5-FU in human serum and urine samples with the Pr:Er/CPE by SWV.

samples	Spiked (10^{-7} M)	Founded[a] (10^{-7} M)	Recovery (%)	RSD (%)	HPLC	Recovery (%)
Urine sample1	0.2	0.194	97.0	1.2	0.202	101
Urine sample2	0.4	0.393	98.2	1.1	0.396	99
Urine sample3	0.6	0.605	100.8	0.8	0.602	100.3
Blood serum sample1	0.3	0.296	98.7	1.2	0.297	99.0
Blood serum sample2	0.5	0.494	98.8	0.9	0.503	100.6
Blood serum sample3	0.7	0.695	99.3	0.8	0.698	99.7

[a] Mean average of four determinations.

4. Conclusions

Given the good electrocatalytic activity of Pr:Er nano-composit in the oxidation of 5-FU, a Pr:Er/CPE was constructed and used in the SWV analysis of 5-FU. The low detection limit (0.98 nM) makes the method an attractive candidate for the trace analysis of the analyte. The developed modified electrode was applied in the analysis of 5-FU in pharmaceutical formulations and low RSDs were recorded. Based on the results of Table 1 the method offers a low detection limit and good sensitivity, together with good reproducibility, short response time, ease of construction and modification of the electrode and the renewability of its surface, which prove it to be a good electrochemical sensor for use in different systems.

Author statement

Ms. Hana Beigizadeh, Mr. Meisam Sadeghpour Karimi acquire the electrochemical analysis. Dr. Ali Sobhani-Nasab Synthesis the nanostructure. Dr. Mehdi Rahimi-Nasrabadi perform the analysis of nanostrucute and **evaluate the whole data**. Dr. Farhad Ahmadi do Funding acquisition and evaluate the electrochemical data, Prof. Yvonne Joseph, Prof. Hermann Ehrlich and Prof. Mohammad Reza Ganjali edit the manuscript and evaluate the procedure and methodologhy and data of the manuscript.

Declaration of Competing Interest

The authors declare that they have no any type of conflict of interest.

Acknowledgements

Authors are grateful to council of Iran University of Medical Sciences for providing financial support to undertake this work.

References

[1] H. Amani, M. Ajami, S. Nasseri Maleki, H. Pazoki-Toroudi, M. Daglia, A.J. Tsetegho Sokeng, A. Di Lorenzo, S.F. Nabavi, K.P. Devi, S.M. Nabavi, Targeting signal transducers and activators of transcription (STAT) in human cancer by dietary polyphenolic antioxidants, Biochimie 142 (2017) 63–79.
[2] S. Tejada, A. Manayi, M. Daglia, S.F. Nabavi, A. Sureda, Z. Hajheydari, O. Gortzi, H. Pazoki-Toroudi, S.M. Nabavi, Wound healing effects of curcumin: a short review, Curr. Pharm. Biotechnol. 17 (2016) 1002–1007.
[3] H. Pazoki-Toroudi, M. Rahgozar, A. Bakhtiarian, B. Djahanguiri, Potassium channel modulators and indomethacin-induced gastric ulceration in rats, Scand. J. Gastroenterol. 34 (1999) 962–966.
[4] A. Firooz, N. Bouzari, F. Mojtahed, H. Pazoki-Toroudi, M. Davoudi, Y. Dowlati, Topical immunotherapy with diphencyprone in the treatment of extensive and/or long-lasting alopecia areata, J. Eur. Acad. Dermatol. Venereol. 19 (2005) 393–394.
[5] D.B. Longley, D. Paul Harkin, P.G. Johnston, 5-fluorouracil: mechanisms of action and clinical strategies, Nat. Rev. Cancer 3 (2003) 330–338.
[6] D. Lima, G.N. Calaça, A.G. Viana, C. Pessôa, Porphyran-capped gold nanoparticles modified carbon paste electrode: a simple and efficient electrochemical sensor for the sensitive determination of 5-fluorouracil, Appl. Surf. Sci. 427 (2018) 742–753.
[7] B.B. Prasad, D. Kumar, R. Madhuri, M.P. Tiwari, Nonhydrolytic sol–gel derived imprinted polymer–multiwalled carbon nanotubes composite fiber sensors for electrochemical sensing of uracil and 5-fluorouracil, Electrochim. Acta 71 (2012) 106–115.
[8] C.G. Zambonin, A. Guerrieri, F. Palmisano, Simultaneous determination of 5′-deoxy-5-fluorouridine, 5-fluorouracil and 5,6-dihydro-5-fluorouracil in plasma by gas chromatography-mass spectrometry, Anal. Chim. Acta 329 (1996) 143–152.
[9] Y. Gu, R. Lu, D. Si, Ch. Liu, Determination of 5-fluorouracil in human plasma by high-performance liquid chromatography (HPLC), Trans. Tianjin Univ. 16 (2010) 167–173.
[10] J.T. Yu, K.J. Bisceglia, E.J. Bouwer, A.L. Roberts, M. Coelhan, Determination of pharmaceuticals and antiseptics in water by solid-phase extraction and gas chromatography/mass spectrometry: analysis via pentafluorobenzylation and stable isotope dilution, Anal. Bioanal. Chem. 403 (2012) 583–591.
[11] V.P. Pattar, Sh.T. Nandibewoor, Electroanalytical method for the determination of 5-fluorouracil using a reduced graphene oxide/chitosan modified sensor, RSC Adv. 5 (2015) 34292–34301.
[12] D. Koyuncu Zeybek, B. Demir, B. Zeybek, S. Pekyardimci, A sensitive electrochemical DNA biosensor for antineoplastic drug 5-fluorouracil based on glassy carbon electrode modified with poly(bromocresol purple), Talanta 144 (2015) 793–800.
[13] F. Ahmadi, B. Jafari, Voltammetry and spectroscopy study of in vitro interaction of fenitrothion with DNA, Electroanalysis 23 (2011) 675–682.
[14] M.R. Ganjali, M.B. Gholivand, M. Rahimi-Nasrabadi, B. Maddah, M. Salavati-Niasari, F. Ahmadi, Synthesis of a new octadentates Schiff's base and its application in construction of a highly selective and sensitive lanthanum (III) membrane sensor, Sens. Lett. 4 (2006) 356–363.
[15] M. Rahimi-Nasrabadi, A. Khoshroo, M. Mazloum-Ardakani, Electrochemical determination of diazepam in real samples based on fullerene-functionalized carbon nanotubes/ionic liquid nanocomposite, Sens. Actuators B 240 (2017) 125–131.
[16] G. Chen, X. Hao, B.L. Li, H.Q. Luo, N.B. Li, Anodic stripping voltammetric measurement of trace cadmium at antimony film modified sodium montmorillonite doped carbon paste electrode, Sens. Actuators B 237 (2016) 570–574.
[17] K. Skrzypczyńska, K. Kuśmierek, A. Świątkowski, Carbon paste electrodes modified with various carbonaceous materials for the determination of 2, 4-dichlorophenoxyacetic acid by differential pulse voltammetry, J. Electroanal. Chem. 766 (2016) 8–15.
[18] J.H. Luo, X.X. Jiao, N.B. Li, H.Q. Luo, Sensitive determination of cd (ii) by square wave anodic stripping voltammetry with in situ bismuth-modified multiwalled carbon nanotubes doped carbon paste electrodes, J. Electroanal. Chem. 689 (2013) 130–134.
[19] Y. Temerk, H. Ibrahim, N. Farhan, Square wave adsorptive stripping voltammetric determination of anticancer drug nilutamide in biological fluids using cationic surfactant cetyltrimethylammonium bromide, Anal. Methods 7 (21) (2015) 9137–9144.
[20] M. Ibrahim, Y. Temerk, H. Ibrahim, M. Kotb, Indium oxide nanoparticles modified carbon paste electrode for sensitive voltammetric determination of aromatase inhibitor formestane, Sens. Actuators B 209 (2015) 630–638.
[21] M. Rahimi-Nasrabadi, S.M. Pourmortazavi, M.R. Ganjali, P. Norouzi, F. Faridbod, M. Sadeghpour Karimi, Statistically optimized synthesis of dyspersium tungstate nanoparticles as photocatalyst, J. Mater. Sci. 27 (2016) 12860–12868.
[22] F. Ahmadi, M. Rahimi-Nasrabadi, M. Behpour, Synthesis Nd_2TiO5 nanoparticles with different morphologies by novel approach and its photocatalyst application, J. Mater. Sci. 28 (2017) 1531–1536.
[23] M. Rahimi-Nasrabadi, S.M. Pourmortazavi, M. Aghazadeh, M.R. Ganjali, M. Sadeghpour Karimi, P. Novrouzi, Optimizing the procedure for the synthesis of nanoscale gadolinium(III) tungstate as efficient photocatalyst, J. Mater. Sci. 28 (2017) 3780–3788.
[24] M. Rostami, M. Rahimi-Nasrabadi, M.R. Ganjali, F. Ahmadi, A. Fallah Shojaei, M. Delavar Rafiee, Facile synthesis and characterization of TiO_2-graphene-$ZnFe_{2-x}TbxO_4$ ternary nano-hybrids, J. Mater. Sci. 52 (2017) 7008–7016.
[25] M. Eghbali-Arani, A. Sobhani-Nasab, M. Rahimi-Nasrabadi, S. Pourmasoud, Green synthesis and characterization of $SmVO_4$ nanoparticles in the presence of carbohydrates as capping agents with investigation of visible-light photocatalytic properties, J. Electron. Mater. 47 (2018) 3757–3769.
[26] A. Sobhani-Nasab, S. Pourmasoud, F. Ahmadi, M. Wysokowski, T. Jesionowski, H. Ehrlich, M. Rahimi-Nasrabadi, Synthesis and characterization of MnWO4/$TmVO_4$ ternary nano-hybrids by an ultrasonic method for enhanced photocatalytic activity in the degradation of organic dyes, Mater. Lett. 238 (2019) 159–162.
[27] A. Sobhani-Nasab, H.R. Naderi, M. Rahimi-Nasrabadi, M.R. Ganjali, Evaluation of supercapacitive behavior of samarium tungstate nanoparticles synthesized via sonochemical method, J. Mater. Sci. Mater. Electron. 28 (2017) 8588–8595.
[28] M. Rahimi-Nasrabadi, S.M. Pourmortazavi, M. Aghazadeh, M.R. Ganjali, M. Sadeghpour Karimi, P. Novrouzi, Samarium carbonate and samarium oxide; synthesis, characterization and evaluation of the photo-catalytic behavior, J. Mater.

Sci. Mater. Electron. 28 (2017) 5574–5583.
[29] S.M. Peymani-Motlagh, A. Sobhani-Nasab, M. Rostami, H. Sobati, M. Eghbali-Arani, M. Fasihi-Ramandi, M. Reza Ganjali, M. Rahimi-Nasrabadi, Assessing the magnetic, cytotoxic and photocatalytic influence of incorporating Yb^{3+} or Pr^{3+} ions in cobalt–nickel ferrite, J. Mater. Sci. 30 (2019) 6902–6909.
[30] H. Ibrahim, Y. Temerk, N. Farhan, Electrochemical sensor for individual and simultaneous determination of guanine and adenine in biological fluids and in DNA based on a nano-In–ceria modified glassy carbon paste electrode, RSC Adv. 6 (93) (2016) 90220–90231.
[31] M. Rahimi-Nasrabadi, V. Pourmohamadian, M. Sadeghpour Karimi, H.R. Naderi, M.A. Karimi, K. Didehban, M.R. Ganjali, Assessment of supercapacitive performance of europium tungstate nanoparticles prepared via hydrothermal method, J. Mater. Sci. 28 (2017) 12391–12398.
[32] M. Rahimi-Nasrabadi, S.M. Pourmortazavi, M.R. Ganjali, P. Norouzi, Optimizing the synthesis procedure and characterization of terbium(III) tungstate nanoparticles as high performance photocatalysts, J. Mater. Sci. Mater. Electron. 28 (2017) 9724–9731.
[33] M. Rahimi-Nasrabadi, S.M. Pourmortazavi, M.R. Ganjali, P. Novrouzi, F. Faridbod, M. Sadeghpour Karimi, Preparation of dysprosium carbonate and dysprosium oxide efficient photocatalyst nanoparticles through direct carbonation and precursor thermal decomposition, J. Mater. Sci. Mater. Electron. 28 (2017) 3325–3336.
[34] M. Rahimi-Nasrabadi, S.M. Pourmortazavi, M. Sadeghpour Karimi, M. Aghazadeh, M.R. Ganjali, P. Norouzi, Erbium(III) tungstate nanoparticles; optimized synthesis and photocatalytic evaluation, J. Mater. Sci. 28 (2017) 6399–6406.
[35] S.M. Pourmortazavi, M. Rahimi-Nasrabadi, M. Aghazadeh, M.R. Ganjali, M. Sadeghpour Karimi, P. Norouzi, Synthesis, characterization and photocatalytic activity of neodymium carbonate and neodymium oxide nanoparticles, J. Mol. Struct. 1150 (2017) 411–418.
[36] M. Rahimi-Nasrabadi, S.M. Pourmortazavi, M. Aghazadeh, M.R. Ganjali, M. Sadeghpour Karimi, P. Norouzi, Fabrication, characterization and photochemical activity of ytterbium carbonate and ytterbium oxide nanoparticles, J. Mater. Sci. 28 (2017) 9478–9588.
[37] M. Rahimi-Nasrabadi, S.M. Pourmortazavi, M. Aghazadeh, M.R. Ganjali, M. Sadeghpour Karimi, P. Norouzi, Synthesis of nano-structured lanthanum tungstates photocatalysts, J. Mater. Sci. 28 (2017) 7600–7608.
[38] S.M. Pourmortazavi, M. Rahimi-Nasrabadi, B. Larijani, M. Sadeghpour Karimi, S. Mirsadeghi, Electrochemical synthesis of cobalt disulfide nanoparticles and their application as potential photocatalyst, J. Mater. Sci. 29 (2018) 13833–13841.
[39] M. Rahimi-Nasrabadi, S.M. Pourmortazavi, M. Sadeghpour Karimi, M. Aghazadeh, M.R. Ganjali, P. Norouzi, Statistical optimization of experimental parameters for synthesis of two efficient photocatalyst: erbium carbonate and erbium oxide nanoparticles, J. Mater. Sci. Mater. Electron. 28 (2017) 15224–15232.
[40] S.M. Pourmortazavi, M. Rahimi-Nasrabadi, M. Aghazadeh, M.R. Ganjali, M. Sadeghpour Karimi, P. Norouzi, Synthesis of Sm_2 $(WO_4)_3$ nanocrystals via a statistically optimized route and their photocatalytic behavior, Mater. Res. Express 4 (2017) 035012.
[41] A.J. Bard, L.R. Faulkner, Electrochemical Methods: Fundamentals and Applications, 2nd ed., (2001).
[42] Ch. Brett, A.M.O. Brett, Electrochemistry: Principles, methods, and Applications, 1st ed., Oxford University Press, 1993.
[43] E. Laviron, General expression of the linear potential sweep voltammogram in the case of diffusionless electrochemical systems, J. Electroanal. Chem. Interfacial Electrochem. 101 (1979) 19–28.
[44] S.D. Bukkitgar, N.P. Shetti, Electrochemical behavior of an anticancer drug 5-fluorouracil at methylene blue modified carbon paste electrode, Mater. Sci. Eng. C 65 (2016) 262–268.
[45] X. Hua, X. Hou, X. Gong, G. Shen, Electrochemical behavior of 5-fluorouracil on a glassy carbon electrode modified with bromothymol blue and multi-walled carbon nanotubes, Anal. Methods 5 (2013) 2470–2476.
[46] S.R. S.ataraddi, S.T. Nandibewoor, Voltammetric-oxidation and determination of 5-flurouracil and its analysis in pharmaceuticals and biological fluids at glassy carbon electrode mediated by surfactant cetyltrimethyl ammonium bromide, DER Pharma Chem. 3 (2011) 253–265.
[47] S. Wang, S. Fu, H. Ding, Determination of 5-fluorouracil using disposable gold nanoparticles modified screen-printed electrode, Sens. Lett. 10 (2012) 974–978.
[48] A.F. Shojaei, K. Tabatabaeian, S. Shakeri, F. Karimi, A novel 5-fluorouracile anticancer drug sensor based on $ZnFe_2O_4$ magnetic nanoparticles ionic liquids carbon paste electrode, Sens. Actuators B. 230 (2016) 607–614.
[49] C. Weiluan, S. Yuanyuan, R. Haojun, L. Lei, G. Shengrong, Development and application of a validated gradient elution HPLC method for simultaneous determination of 5-fluorouracil and paclitaxel in dissolution samples of 5-fluorouracil/paclitaxel-co-eluting stents, J. Pharm. Biomed. Anal. 59 (2012) 179–183.